

HIGH PERFORMANCE ANTI-WINDUP FOR ROBOT MANIPULATORS

Federico Morabito,^{†§} Andrew R. Teel^{*‡} and Luca Zaccarian^{†§}

Keywords: Anti-windup, robotics, input saturation

Abstract

In this paper we provide a high performance solution to the anti-windup problem for control systems on saturated fully actuated robot manipulators. Based on the preliminary work of [10], we provide here improved anti-windup laws based on simple and intuitive parameter tuning. Global asymptotic (and local exponential) stability of the arising closed-loops is formally proven and demonstrated on a simulation example. The simulation example also shows dramatic improvements as compared to previous results.

1 Introduction

Actuator saturation is one of the most common unmodeled phenomena in classical control systems. One of the most studied fields where actuator saturation is involved is that of linear control systems for linear plants. In particular, in the past years great deal of attention has been given to the study of the so-called “windup” problem for linear plants, wherein a pre-designed linear controller is known to work very desirably when interconnected to the linear plant but unpredictable behavior and, often, instability occurs if the input saturation effect is taken into account when interconnecting the controller to the plant. For these windup-prone control systems, “anti-windup design” denotes the synthesis of suitable (linear or nonlinear) filters which augment the original linear controller with the goal of

1. preserving the linear response prespecified by the linear closed-loop as long as the saturation limits are never reached by the actuators;
2. guaranteeing as much as possible the recovery of this linear closed-loop response for all other trajectories.

Many useful constructions are nowadays available in the literature for linear anti-windup designs (see, e.g., [4, 8, 3] for some recent surveys).

A parallel reasoning can be made when dealing with more complicated control systems, such as a nonlinear controller interconnected to a robotic manipulator. In this case, the plant without input saturation is already nonlinear but is characterized by useful properties (such as the feedback linearizability) which provide constructive techniques for high performance nonlinear control laws. When saturation is taken into account, these

control laws exhibit a similar behavior to the “windup” phenomenon widely studied in linear control systems. Indeed, the windup effects on nonlinear saturated control systems is often even worse than the parallel effect in the linear control setting. When dealing with nonlinear plants, we can no longer refer to “desirable linear responses” and the two above mentioned anti-windup requirements need to be rephrased as follows:

1. preserve the unconstrained response arising from the direct interconnection between the nonlinear plant and the nonlinear controller (without saturation) as long as the plant input does not exceed the saturation limits;
2. guarantee as much as possible the recovery of this unconstrained (nonlinear) closed-loop response for all other trajectories.

In this paper we address the anti-windup design problem for robotic manipulators. In recent years, this problem has been indirectly tackled in the context of anti-windup design for nonlinear plants. In the discrete-time setting, nonlinear anti-windup design techniques have been applied to nonlinear systems in [2, 1]. Interesting results related to the nonlinear anti-windup problem can also be found in [12, 5], where the attention is restricted to SISO nonlinear plants. MIMO nonlinear plants are considered in [7, 6]. However, only local stability results are proven in [6] and restrictions on the local design are necessary in some cases. In [7], the open-loop plant and other subsystems internal to the closed-loop are constrained to be asymptotically stable. Differently from the papers listed above we explicitly address the problem of anti-windup design for saturated robotic manipulators here with the goal in mind of guaranteeing high-performance global results. In particular, we improve our work recently appeared in [10], where the ideas of [11] were employed to provide explicit anti-windup constructions for Euler-Lagrange systems.

The goal of this paper is twofold. The first goal is to clarify the construction suggested in [10] when applied to fully actuated robotic manipulators (which is the main application field for the theory in [10]). The second and main goal is to revisit and improve the anti-windup laws of [10] to guarantee extreme performance levels on the saturated closed-loop system with anti-windup augmentation. To provide compensation laws that are simple to apply, we explain how the anti-windup gains should be selected and tuned for achieving high performance compensation on generic robot manipulators. Indeed, the parameter tuning boils down to the selection of a proportional and a derivative gain for each degree of freedom of the robotic structure. The paper is structured as follows: in Section 2 we describe the anti-windup problem and introduce some useful notation; in Section 3 we first report on the results of [10] and then extend these results to allow for high-performance anti-windup designs; in Section 4 we discuss useful characterizations of the anti-windup performance and, based on these, we provide a simple selection strategy for the anti-windup parameters. Finally, in Section 5 we show the dramatic performance

*Department of Electrical and Computer Engineering, University of California, Santa Barbara, CA 93106; Tel: (805) 893-3616; Fax: (805) 893-3262; teel@ece.ucsb.edu

†Dipartimento di Informatica, Sistemi e Produzione, University of Rome, Tor Vergata, 00133 Rome, Italy; Tel: +39 06 7259-7429; Fax: +39 06 7259-7460; email: zack@disp.uniroma2.it

‡Research supported in part by AFOSR grant number F49620-00-1-0106.

§Research supported in part by MIUR and ASI.

improvements of the new anti-windup law as compared to the previous one on a simulation example taken from [10].

2 Problem data

We will consider in this paper fully actuated rigid robot manipulators taking into account the actuator limits affecting their input signals. Given a manipulator belonging to this family, denoting by $q \in \mathbb{R}^n$ the n joint position variables and by $\dot{q} \in \mathbb{R}^n$ the corresponding velocity variables, it is well known that the manipulator can be modeled by the following dynamic equations:

$$I(q)\ddot{q} + C(q, \dot{q})\dot{q} + R(q)\dot{q} + h(q) = u, \quad (1)$$

where $I(q)$ is the generalized inertia matrix, $C(q, \dot{q})\dot{q}$ represents the generalized centrifugal and Coriolis terms, $h(q)$ is the vector of gravitational forces, the function $R(q)\dot{q}$ represents the friction forces and u represents the external forces/torques applied at the robot joints.

The following basic assumption on the regularity of the matrices characterizing (1) will be necessary to prove the main results of this paper. These assumptions are standard properties characterizing mechanical systems.

Assumption 1 *The following properties hold:*

1. the generalized inertia matrix $q \mapsto I(q)$ is continuously differentiable, symmetric and there exist positive numbers λ_M and λ_m such that $\lambda_m Id \leq I(q) \leq \lambda_M Id$ for all $q \in \mathbb{R}^n$ (where Id denotes the identity);
2. the function $(q, \dot{q}) \mapsto C(q, \dot{q})\dot{q}$ is locally Lipschitz;
3. the vector of gravitational forces $q \mapsto h(q)$ is locally Lipschitz;
4. the dissipation matrix $q \mapsto R(q)$ is locally Lipschitz and positive semidefinite.

For the robotic manipulator (1), under Assumptions 1 and 2, we will assume in this paper that a (nonlinear) controller has been designed such that, when connected in feedback with the robot *without* input saturation, global asymptotic and local exponential stability of the arising closed-loop is guaranteed. One such controller is the following feedback linearizing controller with PID action (also known as “computed torque” controller), which is able to induce linear closed-loop behavior (therefore global exponential stability) when saturation is not present:

$$\begin{aligned} \dot{x}_c &= q - r \\ u &= I(q) \left(-K_p(q - r) - K_d\dot{q} - K_i x_c \right) \\ &+ C(q, \dot{q})\dot{q} + R(q)\dot{q} + h(q), \end{aligned} \quad (2)$$

where $x_c \in \mathbb{R}^n$ is the state of the controller and K_p, K_d, K_i are suitable square matrices (typically diagonal) chosen in such a way that the matrix $\begin{bmatrix} 0 & I & 0 \\ -K_i & -K_p & -K_d \end{bmatrix}$, describing the (linear) closed-loop (1), (2), is Hurwitz. Based on the value of the reference input $r \in \mathbb{R}^n$, the controller (2) is able to globally asymptotically stabilize the position $(q, \dot{q}) = (r, 0)$ when interconnected to the robot (1).

For simplicity, throughout this paper we will always use the controller (2). However, the results provided in [10], summarized and extended in the next sections, apply to any control system which induces global asymptotic stability and local exponential stability on the closed-loop without input saturation.

In this paper we will characterize the input nonlinearity of (1) as a symmetric decentralized saturation function. This characterization aims at describing the presence of a pool of actuators, one at each joint of the robotic structure, each of them associated with a maximum torque/force effort m_i attainable from the related power unit/motor combination. Therefore, the saturation function $\text{sat}(\cdot) : \mathbb{R}^n \rightarrow \mathbb{R}^n$ is decentralized and enforces the saturation levels $m_i, i = 1, \dots, n$ on the input channels. The approach that we propose could also be applied to non symmetric saturations, however for simplicity of notation we only consider the symmetric case here.

Since the control input of the robotic system (1) is bounded by the presence of the saturation nonlinearity, suitable lower bounds on the saturation levels $m_i, i = 1, \dots, n$ need to be imposed to guarantee that the actuators have enough power to sustain the robotic structure against the acceleration arising from the gravitational effects. To this aim, we formalize in the following assumption the requirement that the actuators are powerful enough to be able to compensate the gravitational forces in any configuration of the robot (corresponding to a selection of $q \in \mathbb{R}^n$) with zero velocity. Note that this condition is also necessary when wanting to stabilize any configuration of the robot.

Assumption 2 *Given the gravitational forces vector $h(\cdot)$ of the robotic system (1) and the saturation limits $m_i, i = 1, \dots, n$, the following inequalities hold:*

$$h_{Mi} := \sup_{q \in \mathbb{R}^n} |h(q)| < m_i, \quad i = 1, \dots, n. \quad (3)$$

The windup problem discussed in the Introduction arises when the controller (2) is no longer interconnected to the plant *without* input saturation but saturation is accounted for in the interconnection. The typical effects of saturation on the closed-loop behavior is to preserve the desirable unconstrained behavior when signals are small enough not to reach the saturation limits and to cause performance and (often) stability loss when signals become large enough so that the saturation enforces modifications at the plant control input.

3 A nonlinear anti-windup solution

3.1 Prior work

In this section, we summarize the contribution of [10], when applied to robotic manipulators (which can be described by equations of the type (1)). As shown in Figure 1, this anti-windup solution corresponds to the insertion of an “anti-windup compensator” as an augmentation to the original control law (2). According to Figure 1, in the following we will denote by $x := (q, \dot{q}) \in \mathbb{R}^{2n}$ the state of the robot, by $y_c \in \mathbb{R}^n$ the controller output, by $u = \text{sat}(y_c + v_1) \in \mathbb{R}^n$ the robot torque/force input and by $u_c = x + v_2 \in \mathbb{R}^{2n}$ the measurement input of the controller. The anti-windup compensator has access to the plant’s state and input and to the controller output. The authority of the anti-windup compensator, which allows to add modifications to the original closed-loop, consists in two compensation signals v_1 and v_2 which are injected at the controller output and input, respectively. Based on the general approach in [10], when considering robot manipulators, we can provide simplified expressions of the compensation laws implemented in the “anti-windup compensator” block of Figure 1.

In particular, denoting the anti-windup compensator's state by $x_e := (q_e, \dot{q}_e) \in \mathbb{R}^{2n}$, its dynamics can be written as

$$\begin{aligned} \ddot{q}_e = & I^{-1}(q) (\text{sat}(y_c + v_1) - C(q, \dot{q})\dot{q} - R(q)\dot{q} - h(q)) \\ & - I^{-1}(q - q_e)(y_c - C(q - q_e, \dot{q} - \dot{q}_e)(\dot{q} - \dot{q}_e) \\ & - R(q - q_e)(\dot{q} - \dot{q}_e) - h(q - q_e)). \end{aligned} \quad (4)$$

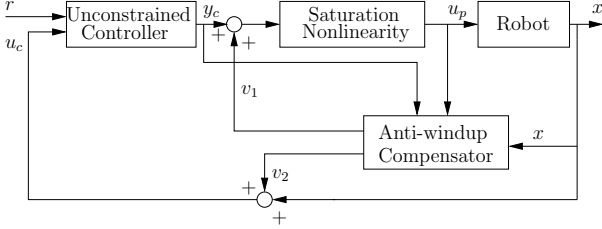


Figure 1: The anti-windup scheme for robot manipulators.

The anti-windup compensator outputs $v_1 \in \mathbb{R}^n$ and $v_2 \in \mathbb{R}^{2n}$ correspond to

$$v_1 = \beta(x, x_e), \quad v_2 = -x_e = -(q_e, \dot{q}_e), \quad (5)$$

where $\beta(\cdot, \cdot) : \mathbb{R}^{2n} \times \mathbb{R}^{2n} \rightarrow \mathbb{R}^n$ is given by

$$\beta(x, x_e) := h(q) - h(q - q_e) - K_g \text{sat}(K_g^{-1} q_e) - K_0 \dot{q}_e. \quad (6)$$

The two matrices K_0 and K_g are positive definite diagonal and they represent the “tuning” parameters of the anti-windup law. The diagonal elements κ_{gi} , $i = 1, \dots, n$ of K_g need to satisfy the following constraints:

$$h_{Mi} + \kappa_{gi} m_i < m_i, \quad i = 1, \dots, n. \quad (7)$$

Note that by definition of h_{Mi} in (3), if Assumption 2 holds, there always exists a positive definite diagonal matrix K_g fulfilling the constraints (7).

The main result of [10] establishes useful properties of the trajectories of the *anti-windup closed-loop system* (1), (2), (4), (5), (6) (whose state will be denoted by (x, x_c, x_e)) when compared to the (ideal) trajectories of the unconstrained closed-loop system (1), (2) (whose state will be denoted using the subscript “ ℓ ”, namely $(x_\ell, x_{c\ell})$). This is formalized in the following theorem (reported without proof).

Theorem 1 [10] *Suppose that Assumptions 1 and 2 hold and the parameters of the compensation law (6) satisfy (7). Given a constant reference signal r , denote by $(x_\ell(t), x_{c\ell}(t))$ the response of the unconstrained closed-loop system (1), (2) starting from the initial conditions $((x_\ell(0), x_{c\ell}(0)))$. Denote also by $u_\ell(t)$ the corresponding controller output. Then the anti-windup closed-loop system (1), (2), (4), (5), (6) is such that*

1. *if $u_\ell(t) = \text{sat}(u_\ell(t))$ for all times and $(x(0), x_c(0), x_e(0)) = (x_\ell(0), x_{c\ell}(0), 0)$, then $(x(t), x_c(t), x_e(t)) = (x_\ell(t), x_{c\ell}(t), 0)$ for all times, namely the unconstrained response is retained;*
2. *defining $x^* := (r, 0)$, there exists a vector $x_c^* \in \mathbb{R}^n$ such that the point $(x^*, x_c^*, 0)$ is globally asymptotically stable and locally exponentially stable.*

Theorem 1 establishes two important properties of the anti-windup closed-loop system (1), (2), (4), (5), (6). The first one corresponds to the key constraint of anti-windup construction discussed in the Introduction: the anti-windup compensation preserves the local response of the original (unconstrained) closed-loop whenever the saturation limits are not exceeded

by the unconstrained trajectory. The second property states that the closed-loop with anti-windup augmentation is globally asymptotically stable, thus the instability effects often experienced when control laws such as (2) reach the saturation limits (see Section 5 for a notable example of this phenomenon) are eliminated by the proposed anti-windup augmentation strategy.

3.2 A generalized result

If on one hand the result of the previous section guarantees important properties of our anti-windup augmentation scheme, very little is established about the transient response of the anti-windup closed-loop system after the saturation limits are reached by the actuators: in this case, the only property guaranteed by Theorem 1 (in particular, by item 2) is that the closed-loop trajectories converge to the desired equilibrium point where $q = r$ and $\dot{q} = 0$. Nothing can be concluded, however, about the transient behavior of these trajectories. To allow for high performance selections of the anti-windup compensator parameters (the selection method will be clarified in the following section), we introduce in this section an extension of the anti-windup law of [10] summarized above. In particular, we propose a generalization of the selection for v_1 in (6) as follows:

$$v_1 = \text{sat}(y_c) - y_c + h(q) - h(q - q_e) - K_g \text{sat}(K_g^{-1} K_q q_e) - K_{qd}(q_e, \dot{q}_e) \dot{q}_e, \quad (8)$$

where K_g is a diagonal matrix whose elements still satisfy the constraints (7), K_q is a diagonal positive definite matrix and $K_{qd}(\cdot, \cdot)$ is a decentralized diagonal matrix function whose diagonal function elements $(q_{ei}, \dot{q}_{ei}) \mapsto \kappa_{qdi}(q_{ei}, \dot{q}_{ei})$, $i = 1, \dots, n$ are constant in a neighborhood of the origin and bounded away from zero, and such that the functions $(q_{ei}, \dot{q}_{ei}) \mapsto \kappa_{qdi}(q_{ei}, \dot{q}_{ei}) \dot{q}_{ei}$ are locally Lipschitz for all i .

By suitably generalizing the proof of the main result of [10] (corresponding to Theorem 1 above), the following parallel result can be established for the generalized anti-windup closed-loop system arising from the interconnection between (1), (2), (4), (5) and the new compensation law (8). The proof of the following theorem is omitted because of its similarity with Theorem 1 and due to space constraints.

Theorem 2 *Suppose that Assumptions 1 and 2 hold and the parameters of the compensation law (8) satisfy (7). Then the anti-windup closed-loop system (1), (2), (4), (5), (8) induces the two properties established in Theorem 1.*

Note that the compensation law (8) is a generalization of (6). This generalization allows for significant performance improvements as compared to the results reported in [10] (where the compensation law (6) was employed). To this aim, in the next section we will first characterize mathematically the performance of the anti-windup compensation scheme and then describe suitable selections of the parameters K_g , K_q and $K_{qd}(\cdot, \cdot)$ in (8) that are especially effective at guaranteeing high performance compensation.

4 Improving the anti-windup performance

Following the anti-windup qualitative goal of recovering as much as possible “what the response without input saturation

would be”, the quality of the closed-loop response can be measured in terms of the deviation of the actual plant trajectory x from the corresponding (ideal) unconstrained plant trajectory x_ℓ . In particular, we are interested in the size of the signal $x(t) - x_\ell(t)$ for all positive times (and item 2 of Theorem 1 guarantees that, for any constant reference r , $x(t) - x_\ell(t)$ converge to zero because both these signals converge to the equilibrium $(r, 0)$).

While item 1 of Theorem 1 guarantees that $x(t) - x_\ell(t)$ is identically zero when $u_\ell(\cdot)$ never exceeds the saturation limits, no information about the transient behavior of $x(t) - x_\ell(t)$ is available from the theorem for all other trajectories. On the other hand, based on continuity of trajectories with respect to initial conditions on compact time intervals (this is a standard result of nonlinear systems analysis) and on the GAS property of item 1, it is reasonable to expect that unconstrained trajectories corresponding to control inputs u_ℓ that spend little time (and little energy) outside the saturation limits will correspond to trajectories of the anti-windup closed-loop system such that $x(t) - x_\ell(t)$ is very small (in some sense). For all the remaining trajectories, not much can be concluded about their transient behavior from Theorem 1. For these cases, the following result is a good starting point to monitor and, possibly, make small the size of $x(t) - x_\ell(t)$.

Theorem 3 *Regardless of the selection of v_1 in (5), given any reference signal $r(t), t \geq 0$, denote by $(x_\ell(t), x_{cl}(t))$ the response of the unconstrained closed-loop system (1), (2) starting from the initial conditions $((x_\ell(0), x_{cl}(0)))$ and denote by $(x(t), x_c(t), x_e(t))$ the response of the anti-windup closed-loop system (1), (2), (4), (5) starting from the initial conditions $(x(0), x_c(0), x_e(0)) = (x_\ell(0), x_{cl}(0), 0)$. Then $x_e(t) = x_\ell(t) - x(t), \forall t \geq 0$.*

Proof. Consider the closed-loop (1), (2), (4), (5) and perform the change of coordinates $(x, x_c, x_e) \rightarrow (\tilde{x}, x_c, x_e)$, where $\tilde{x} := x - x_e$. Then, defining $(\tilde{q}, \dot{\tilde{q}}) := \tilde{x}$, after some computation, the following equations are obtained:

$$\begin{cases} \ddot{\tilde{q}} &= -I^{-1}(\tilde{q}) (C(\tilde{q}, \dot{\tilde{q}})\dot{\tilde{q}} + R(\tilde{q})\dot{\tilde{q}} + h(\tilde{q}) - y_c) \\ \dot{x}_c &= \tilde{q} - r \\ y_c &= I(\tilde{q}) \left(-K_p(\tilde{q} - r) - K_d\dot{\tilde{q}} - K_i x_c \right) \\ &+ C(\tilde{q}, \dot{\tilde{q}})\dot{\tilde{q}} + R(\tilde{q})\dot{\tilde{q}} + h(\tilde{q}), \end{cases} \quad (9a)$$

$$\begin{cases} \ddot{q}_e &= I^{-1}(\tilde{q} + q_e) (u - C(\tilde{q} + q_e, \dot{\tilde{q}} + \dot{q}_e)(\dot{\tilde{q}} + \dot{q}_e) \\ &- R(\tilde{q} + q_e)(\dot{\tilde{q}} + \dot{q}_e) - h(\tilde{q} + q_e)) \\ &+ I^{-1}(\tilde{q}) (C(\tilde{q}, \dot{\tilde{q}})\dot{\tilde{q}} + R(\tilde{q})\dot{\tilde{q}} + h(\tilde{q}) - y_c) \\ u &= \text{sat}(y_c + v_1). \end{cases} \quad (9b)$$

The representation (9) for the anti-windup closed-loop system is the cascade of two subsystems. The first one (corresponding to (9a)) of coordinates (\tilde{x}, x_c) driving a second one (corresponding to (9b)) of coordinates x_e . Note that the dynamics (9a) of the first subsystem are coincident with the unconstrained dynamics (1), (2) and that, since $x_e(0) = 0$, then $(\tilde{x}(0), x_c(0)) = (x(0), x_c(0))$. Since the dynamics and the initial conditions are the same, $(\tilde{x}(t), x_c(t)) = (x_\ell(t), x_{cl}(t))$ for all positive times. Therefore, by definition, $x_\ell(t) = \tilde{x}(t) = x(t) - x_e(t)$ for all positive times and the result follows. •

From a performance perspective, the relevance of Theorem 3, stands in the fact that it clarifies the impact of the selection of

v_1 on the error variables $x_e = x - x_\ell$. By virtue of the cascade structure (9) pointed out in the proof of Theorem 3, we can focus on the second dynamics (9b) to study selections of v_1 of the type (8) that are particularly effective at keeping q_e small, so that the actual trajectory q is as close as possible to the (ideal) unconstrained trajectory q_ℓ . Note, however, that the global asymptotic (and local exponential) stability of (9b) is already assured by Theorem 2 for all selections of the parameters that satisfy (7), so we can disregard the stability property (which has already been addressed and proven) and concentrate on performance.

One first thing to point out is the fact that, according to the second equation in (9b), the term y_c acts like a disturbance for the dynamics q_e . This motivates the term $\text{sat}(y_c) - y_c$ in equation (8) which alone leads to highly improved responses (as compared to (6)) in the first instants of the closed-loop response. Indeed, especially in aggressive control systems, y_c often presents very large peaks that result in undesired undershoots at the beginning of the anti-windup closed-loop response. Adding this extra term transforms the disturbance from y_c into $\text{sat}(y_c)$, thus reducing significantly its negative effects.¹

To understand the impact of the selection (8) on the error dynamics (9b), it is useful to substitute v_1 and u in the first equation of (9b). We are especially interested in the dynamics of q_e associated with times where the plant input is not anymore saturated, so that full authority is available for the signal v_1 to suitably drive the state x_e . Therefore, substituting $u = y_c + v_1$ in the first equation of (9b) we get (recall that $q_\ell = q - q_e$):

$$\begin{aligned} \ddot{q}_e &= I^{-1}(q_\ell + q_e) (-K_g \text{sat}(K_g^{-1} K_q q_e) - K_{qd}(q_e, \dot{q}_e) \dot{q}_e) \\ &+ I^{-1}(q_\ell + q_e) (\text{sat}(y_c) - C(q_\ell + q_e, \dot{q}_\ell + \dot{q}_e) (\dot{q}_\ell + \dot{q}_e) \\ &- R(q_\ell + q_e) (\dot{q}_\ell + \dot{q}_e) - h(q_\ell)) - \ddot{q}_\ell \end{aligned}$$

Interestingly enough, it results that when (q_e, \dot{q}_e) is small and $\text{sat}(y_c) = y_c$, by continuity, the second line of the above equation is almost zero and the saturation at the first line is not active. Then we get

$$I(q) \ddot{q}_e \approx -K_g \text{sat}(K_g^{-1} K_q q_e) - K_{qd}(q_e, \dot{q}_e) \dot{q}_e, \quad (10)$$

which describes a dynamic system close to a double integrator controlled by a saturated proportional action and by a derivative action, whose gains are associated with the design parameters K_q and $K_{qd}(\cdot, \cdot)$ (recall that $K_{qd}(\cdot, \cdot)$ is diagonal and strictly positive for all values of its argument, by construction).

Let us denote by $\gamma_E(q_e)$ the equivalent gain associated with the saturation of the proportional action, namely $\gamma_E(\cdot)$ is a diagonal decentralized matrix function which satisfies $K_g \text{sat}(K_g^{-1} K_q q_e) = \gamma_E(q_e) K_q q_e$. Then given a positive definite diagonal matrix K_0 , we select each diagonal element $\kappa_{qdi}(\cdot, \cdot)$ of the decentralized function $K_{qd}(\cdot, \cdot)$ as

$$\kappa_{qdi}(q_{ei}, \dot{q}_{ei}) := \begin{cases} \gamma_{E_i}(q_{ei}) \kappa_{0i}, & \text{if } q_{ei} \dot{q}_{ei} > 0 \\ \kappa_{0i}, & \text{otherwise} \end{cases} \quad (11)$$

so that the by means of $K_{qd}(\cdot, \cdot)$ we can “modulate” the derivative action of the controller based on the depth into saturation of the proportional element.² This modulating action leads

¹One may think that the best strategy is to eliminate completely y_c . However, Theorem 2 couldn't be proven in that case.

²Note that since the operating region of the robot is bounded, by the closed-loop stability established in Theorem 2, also q_e is bounded, therefore the selection (11) is bounded away from zero, as required.

to significant performance improvement when q_e is very large and then, due to the saturation nonlinearity, the proportional term becomes too small as compared to the derivative term in (10). Note that with the selection (8), (11), when the saturation element in (8) is not active, the approximate dynamics (10) transform into the simple dynamics

$$I(q)\ddot{q}_e \approx -K_q q_e - K_0 \dot{q}_e, \quad (12)$$

which suggest that the diagonal elements of K_q and K_0 should be selected in an almost decoupled way (“almost” because of the presence of $I(q)$), with the goal of improving the performance at each joint, following a selection approach similar to the heuristic approach for the selection of linear PD gains.

Summarizing the above, a successful strategy for the selection of v_1 is (8), (11), whose design parameters are three positive definite diagonal matrices K_g , K_q , K_0 . The first parameter, K_g , should always be chosen as large as possible within the design constraints (7) to maximize the authority of the proportional gain in the compensation law (note that $K_g < I$ by definition). The parameters K_q and K_0 should be tuned with the goal of improving the transients at each joint following a quasi decoupled PD tuning strategy.

5 Simulation example

In [10], the effectiveness of the proposed anti-windup law has been tested on a SCARA robot (Selective Compliance Assembly Robot Arm). We use here the same example to emphasize the performance improvement that can be guaranteed when employing the improved anti-windup law given by (8), (11). The SCARA robot has four links. The first two links correspond to a planar robot on the horizontal plane. The third link corresponds to a prismatic joint imposing the tilt of the end effector on the working surface and the last joint is a rotational joint corresponding to the end effector orientation with respect to the vertical rotation axis.

| Link | l_i [m] | M_i [kg] | I_i [kgm ²] | m_i |
|------|-----------|------------|---------------------------|-------|
| 1 | 0.6 | 12 | 0.36 | 55 Nm |
| 2 | 0.4 | 6 | 0.08 | 60 Nm |
| 3 | 1 | 3 | 0.08 | 70 N |
| 4 | 0 | 1 | 0.08 | 25 Nm |

Table 1: Parameters of the SCARA robot.

In Table 1 we report the same parameters used in [10] for our simulations. These parameters have been taken from [9]. Table 1 should be read according to the following notation: l_i is the length of the i -th link, M_i is the total mass of the i -th link (including the actuators’ masses), I_i is the rotational inertia of the i -th link and m_i is the saturation level of the i -th actuator.

The unconstrained controller is a “computed torque” controller of the type (2) with the following selection for the proportional, integral and derivative gains: $K_d = \text{diag}(121.5, 30, 150, 150)$, $K_p = \text{diag}(17.79, 8.25, 24.75, 20.13)$, $K_i = \text{diag}(7.5, 10, 1, 0.5)$. We report on simulations using two different anti-windup constructions. The first one is the original construction of [10], where the control law (6) is used with the selection $K_g = \text{diag}(0.9, 0.9, 0.4, 0.9)$, $K_0 = \text{diag}(7.5, 4.5, 3.5, 2)$. The second simulation corresponds to the new construction (8), (11) with the following selection for the parameters:

$$K_g = \text{diag}(0.9, 0.9, 0.4, 0.9) \quad K_0 = \text{diag}(60, 40, 30, 20) \\ K_q = \text{diag}(280, 70, 70, 70).$$

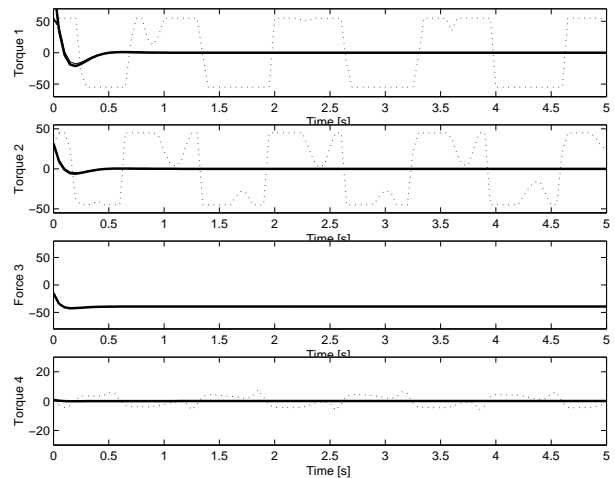


Figure 2: Input responses to the reference (13) of the following closed-loop systems: unconstrained (bold solid), saturated (dotted), anti-windup from [10] (dashed) and new anti-windup law (thin solid).

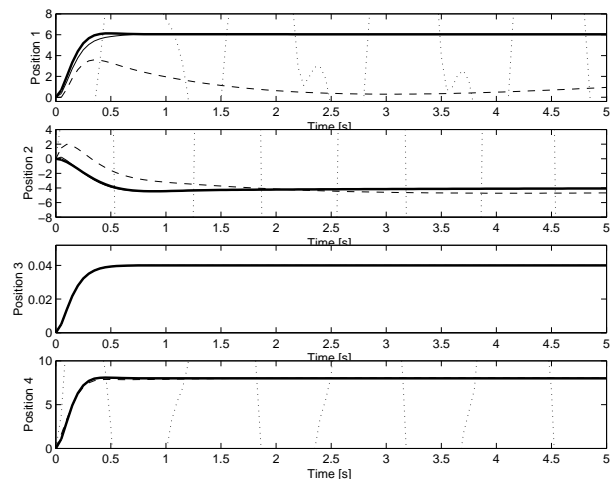


Figure 3: Output responses to the reference (13) of the following closed-loop systems: unconstrained (bold solid), saturated (dotted), anti-windup from [10] (dashed) and new anti-windup law (thin solid).

We first reproduce the same simulation reported in [10], where the reference signal has been selected as

$$r = (6 \text{ deg}, -4 \text{ deg}, 4 \text{ cm}, 4 \text{ deg}). \quad (13)$$

The corresponding responses are reported in Figures 2 and 3.

Note that the new anti-windup law leads to extremely improved performance as compared to the previous law. The corresponding output response is almost coincident with the unconstrained trajectory thus providing almost full recovery of the original linear response. The unpleasant undershoot characterizing the previous anti-windup response from [10] has been completely eliminated and the unconstrained response recovery time reduced to 0.75 seconds (the response from [10] requires approximately 25 seconds to recover the unconstrained response on the first joint). Note also that for this simulation, the saturated

response leads to persistent oscillations (this was already observed in [10]).

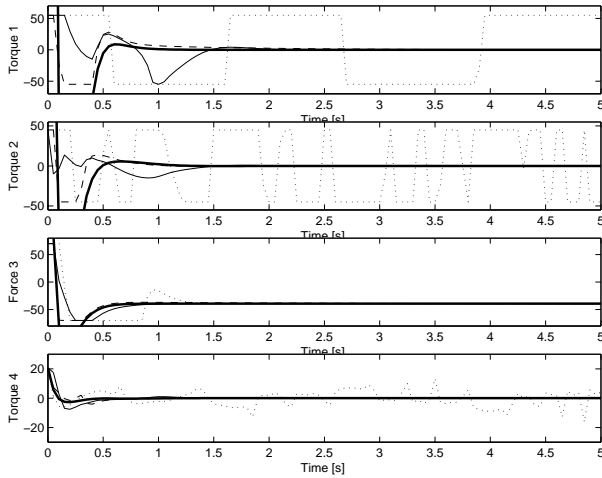


Figure 4: Input responses to the reference (14) of the following closed-loop systems: unconstrained (bold solid), saturated (dotted), anti-windup from [10] (dashed) and new anti-windup law (thin solid).

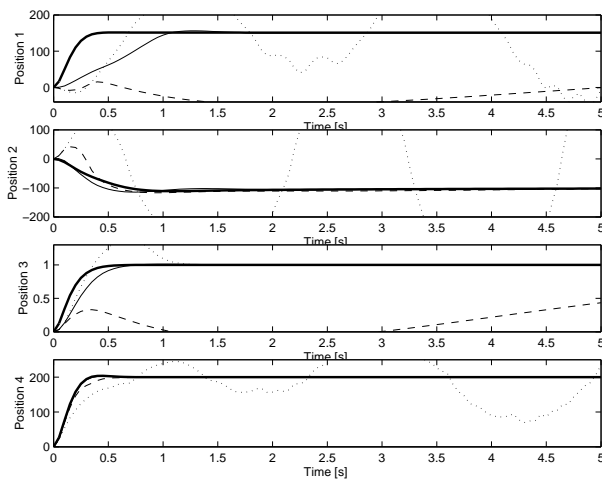


Figure 5: Output responses to the reference (14) of the following closed-loop systems: unconstrained (bold solid), saturated (dotted), anti-windup from [10] (dashed) and new anti-windup law (thin solid).

Next, we report on a different experiment which is aimed at testing the reliability of the anti-windup law when the external reference corresponds to the following unreasonably high level:

$$r = (150 \text{ deg}, -100 \text{ deg}, 1 \text{ m}, 200 \text{ deg}). \quad (14)$$

The resulting trajectories are reported in Figures 4 and 5. In this case, as expectable, the saturated response (dotted) oscillates in an unreasonable way. However, also the anti-windup technique from [10] (dashed) provides poor performance, where the first three joints exhibit unacceptable undershoots and are associated with extremely slow transients. The new strategy (thin solid), instead, provides a response that almost coincides with the unconstrained one in the last three joints, while it is associated with a very fast transient on the first joint, requiring approximately 1.5 seconds to settle on the desired steady state. It is important to emphasize that different transients on each joint

could be imposed by suitably adjusting the diagonal entries of the matrices K_q and K_0 .

6 Conclusions

In this paper we proposed extensions of the anti-windup algorithm of [10], which lead to radical performance improvements of the compensated closed-loop behavior. Among other things, one advantage of the strategy here proposed is that the transient response of the anti-windup closed-loop system can be tuned by acting on simple decoupled proportional and derivative gains. The performance of the closed-loop system has been tested and verified by simulation on a model of a SCARA robot.

References

- [1] D. Angeli and E. Mosca. Command governors for constrained nonlinear systems. *IEEE Trans. Aut. Cont.*, 44(4):816–820, April 1999.
- [2] A. Bemporad. Reference governor for constrained nonlinear systems. *IEEE Trans. Aut. Cont.*, 43(3):415–419, March 1998.
- [3] C. Edwards and I. Postlethwaite. Anti-windup and bumpless-transfer schemes. *Automatica*, 34(2):199–210, 1998.
- [4] R. Hanus. Antiwindup and bumpless transfer: a survey. In *Proceedings of the 12th IMACS World Congress*, volume 2, pages 59–65, Paris, France, July 1988.
- [5] Q. Hu and G.P. Rangaiah. Anti-windup schemes for uncertain nonlinear systems. *IEE proc. Control Theory Appl.*, 147(3):321–329, May 2000.
- [6] N. Kapoor and P. Daoutidis. An observer-based anti-windup scheme for non-linear systems with input constraints. *Int. J. Contr.*, 72(1):18–29, 1999.
- [7] T.A. Kendi and F.J. Doyle III. An anti-windup scheme for multivariable nonlinear systems. *Journal of Process Control*, 7(5):329–343, 1997.
- [8] M.V. Kothare, P.J. Campo, M. Morari, and N. Nett. A unified framework for the study of anti-windup designs. *Automatica*, 30(12):1869–1883, 1994.
- [9] G. Mester. Adaptive force and position control of rigid-link flexible-joint SCARA robots. In *Proc. of the IEEE Industrial Electronics Conference*, volume 3, pages 1639–1644, Bologna (Italy), September 1994.
- [10] F. Morabito, A.R. Teel, and L. Zaccarian. Anti-windup design for Euler-Lagrange systems. In *IEEE Conference on Robotics and Automation*, pages 3442–3447, Washington (DC), USA, May 2002.
- [11] A.R. Teel and N. Kapoor. Uniting local and global controllers. In *Proc. 4th ECC*, Brussels, Belgium, July 1997.
- [12] S. Valluri and M. Soroush. Input constraint handling and windup compensation in nonlinear control. In *Proceedings of the American Control Conference*, pages 1734–1738, Albuquerque (NM), USA, June 1997.